

The Sun's Shape and Brightness

J.R. Kuhn^{1,2} & *R. I. Bush*³ & *X. Scheick*⁴ & *P. Scherrer*³

(1) - Michigan State University

East Lansing-MI-48823

(2) - National Solar Observatory

Sunspot-NM-88349

(3) - Stanford University

Stanford-CA

(4) - Jackson Community College

Jackson-MI-49201

Small departures from sphericity of the Sun can be used as sensitive probes of the solar interior. In particular, asphericity in the effective surface temperature (visible as a solar latitude surface brightness dependence), may be caused by differences between the vertical and horizontal turbulent convective flows¹ in the solar interior. Measuring these temperature variations therefore enables us to investigate the process of convection within stars – an important problem, as it is the convection zone which drives the 11 (and 22) year solar cycle. This remains one of the most mysterious aspects of the Sun. Moreover, variations in the solar luminosity may be related to changes in conditions near the base of the convection zone² that result from the magnetic (sunspot) cycle³. Here we report satellite data that show that the Sun's shape and temperature vary with latitude in an unexpectedly complex form. Although the solar oblateness shows no evidence of changing with the solar cycle, we detect a significant hexadecapole shape term which may vary.

We also observe a 1.5°K latitudinal surface temperature variation; we accordingly suggest that sensitive brightness observations may also record the surface “shadow” of solar cycle changes occurring in the deep solar interior.

Measurements of the shape of the sun, and in particular the solar oblateness, have been published and debated for nearly a century.⁴ Interest in the solar oblateness over the last 35 years was kindled by Dicke and collaborators’ measurements⁵, which suggested that General Relativity may be seriously “incomplete.” Subsequent data^{6–10} did not confirm these results although they have, on occasion, been interpreted as evidence that the Sun’s shape varies over solar cycle timescales.¹¹ Such a variation, should it be confirmed, would require unexpectedly large solar interior rotation, or density, changes to occur over only a few years. This would have a profound effect on our understanding of the solar cycle.

The photometric and astrometric data described here were obtained with the Michelson Doppler Imager (MDI) experiment¹² on 19 March 1996 and 20 March 1997. To measure the limb shape and brightness we decompose the solar limb position and brightness (obtained from full-disk MDI 1024x1024 pixel “continuum” CCD images) into a linear combination of low order Legendre Polynomials (P_l) of the form $\sum_{l=0,2,4} c_l P_l(\cos \theta')$ (where θ' is the solar colatitude). The $l = 2$ term corresponds to a quadrupolar distortion (the “oblateness”). Both the quadrupole and hexadecapole ($l = 4$) shape terms are affected by the solar gravitational potential field and the solar rotation (and differential rotation).

It is critical that the spacecraft, and therefore the MDI optics, be rotated through 360 degrees by small angular increments, since the data must be analysed by a “phase modulation” technique to extract the small solar limb shape and brightness signal from the much larger instrumental noise background. Although we achieve accuracy at the level of about half a kilometer

in the limb shape, *temporal variations* of higher angular harmonics of the limb shape have been measured from MDI data with the even greater sensitivity of 10 microarcseconds (corresponding to a few meters at the solar limb) over a two month duration¹³.

The 1996 observations were obtained from a SOHO spacecraft commissioning roll, which included 90 degree roll angle increments with about 60 minute dwell at each stop. The 1997 roll was performed in increments of 30 degrees with a 25 minute dwell at each stop. The 1996 measurements were obtained without the active MDI image stabilization system which uses an active tip-tilt mirror because of uncertainties in the spacecraft pointing performance. During the 1997 roll, however, the MDI image stabilization system maintained the solar image position to better than 0.001 pixels. Our best data were obtained in 1997, in part because the 12 position roll provided a measurement of higher shape harmonics and the limb brightness signal (which is dominated by higher angular overtones). In addition, the image stabilization system reduced the spacecraft vibration noise observed in the 1997 measurements by over an order of magnitude.

Limb shape and brightness information is derived from a 6 pixel wide annulus which contains the solar limb of the MDI continuum data. All of these pixel data are used to derive a mean limb darkening function (LDF) $L(r)$ for each image. The annular data is then divided into $i = 1, \dots, 512$ angular bins, $2\pi/512$ radians wide, with $j = 1, \dots, N_i$ data values ($N_i \approx 35$ pixels) in each bin centered at angle θ_i . Let $d_i(j)$ be the continuum data for pixel j in bin i , where $r_i(j)$ is the distance of pixel j to the center of the image. Then the average limb displacement at θ_i is determined by a first order least-squares fit of the data from bin i , $d_i(j)$, to the spatially shifted empirical function, $L(r_i(j) - \beta_i)$ (varying β_i). Thus, the relative solar limb position (β_i) is derived for each of 512 position angles around the limb. The local limb “brightness” is derived from a least-squares fit of the residual

brightness $d_i(j) - L(r_i(j) - \beta_i)$ to $\alpha_i L(r_i(j) - \beta_i)$ (varying α_i). Thus, the α_i parameters describe a least-squares estimate of the local intensity scaling factor by which a given limb angle LDF is “brighter.”

The α_i and β_i parameters approximately measure local limb brightness and displacement. This interpretation is approximate because these coefficients are not physically or computationally orthogonal. Furthermore, the limb darkening function may change shape in a more complicated way than we have parametrized, and in response to physical changes in the outer solar atmosphere. Lites¹⁴ has computed specific LDF’s for a variety of perturbations. For example, changes in the solar granulation convection, or the response of the atmosphere to the 5-min oscillations can be reasonably approximated as a scaling and shift of the mean LDF. The detailed physical interpretation of small LDF variations is a fundamental concern for all past and present limb observations and the detection of both limb brightness and shape changes indicates that a more detailed investigation of the LDF variations is warranted.

For MDI the limiting astrometric statistical noise source is small-scale photometric gain variations caused by the detector and optics – accurate differential gain (“flat-field”) calibration of the data is essential. We used a least-squares technique to derive this calibration that involves displacing the telescope and image.¹⁵ The MDI flat-field used in this analysis was computed from observations taken in February 1996 and achieved a relative pixel-pixel photometric calibration which is accurate to better than 1%.

The analysis of each satellite roll sequence is performed separately and we label $\alpha_k(\theta_i)$ and $\beta_k(\theta_i)$ as the coefficients derived from roll position, k . Note that the instrumental optical distortion and photometric uncertainties have amplitudes of order 0.1 pixel (one pixel subtends 1.96”) and 1%, and the solar contributions are much smaller than these terms. Since the detector (and our reference coordinate frame) rotates with the instrument while the solar

contribution does not, the data from a given spacecraft roll angle, ω_k , is well described by $\alpha_k(\theta_i) = B(\theta_i) + I_b(\theta_i - \omega_k)$ and $\beta_k(\theta_i) = S(\theta_i) + I_s(\theta_i - \omega_k)$ where $B(\theta)$ and $S(\theta)$ are the solar contributions to the brightness and shape signals at limb angle θ , and I_b and I_s are the corresponding instrumental contributions. Our sun-centered coordinate frame is oriented so that $\theta = 0$ corresponds to the west equatorial limb with positive angles increasing toward the solar north pole. In Figure 1 we show how an algorithm, similar to phase sensitive detection techniques used in timeseries analysis, allows the separation of the low order harmonics of the solar signals ($B(\theta)$ and $S(\theta)$) from the instrumental noise contributions (I_s and I_b).

Fitting the 1997 $S(\theta)$ results to the above Legendre expansion gives $c_2 = -5.18 \pm 0.44$, and $c_4 = 1.37 \pm 0.54$ milliarcsec. Here we have assumed that the distortion is aligned with the rotation axis to correct for the 6° inclination of the solar axis out of the image plane (by scaling c_2 by 1.02 and c_4 by 1.05). From the ‘F-test’ we must conclude that the P_4 term is well constrained by the observations as it significantly improves the reduced χ_r^2 from the oblateness-only fit at better than the 99% confidence level. Lydon and Sofia⁹ also attempted to measure this shape term in 1992 and 1994 and obtained -0.40 ± 0.44 milliarcsec – consistent with zero, and significantly different from the $l = 4$ term we derive. While the SoHO data yield the first evidence for a non-zero solar hexadecapole moment, the earlier measurements suggest that the Sun’s high order shape may change in time.

The 1996 data give consistent but noisier results, $c_2 = -6.00 \pm 0.80$ milliarcsec (in 1996 c_4 was indeterminate). The weighted average of our 1996 and 1997 data yield $c_2 = -5.38 \pm 0.39$ milliarcsec (the apparent solar radius was $972''$). Figure 2 summarizes the status of many of the oblateness observations from the last 35 years. In contrast to the $l = 4$ shape measurements, the new MDI data, combined with the most recent results from ref. 9 and 10, rule out any 11 year variability in c_2 larger than about 0.5 milliarcsec.

Figure 3 shows that the limb surface brightness, $B(\theta)$, varies with solar latitude. We express this fluctuation in terms of a photometric color temperature variation by scaling $B(\theta)$ by $T_{\odot}/4$ (taking $T_{\odot}=5700\text{K}$ for the effective color temperature). The Princeton-Michigan State-Caltech oblateness/limb photometer had the required accuracy to measure comparably small limb temperature changes, but averaged in relatively larger diametrically opposed limb regions. That experiment³ also found a minimum in the solar limb temperature near ± 55 degrees latitude. The MDI brightness profile obtained here is consistent with those earlier results.

The existence of a surface brightness variation (like the polar brightening in Fig. 3) that is not directly associated with photospheric magnetic fields is characteristic of most global models of the solar differential rotation. Yet, these data show that both the solar shape and brightness are more complicated than a simple quadrupole. It remains to be seen, in detail, what the implications are for our understanding of stellar convection, differential rotation, and the solar cycle. If the tiny brightness variations we now see at the surface do “shadow” the deep convection zone boundary (cf. ref. 2), then we can expect to detect a change in this temperature structure as the solar cycle evolves. Future MDI/SoHO observations should be able to confirm or refute this view.

Address correspondence or request for materials to jkuhn@solar.stanford.edu.

References

1. Durney, B.R., and Roxburgh, I., Inhomogeneous Convection and the Equatorial Acceleration *Sol. Phys.* **16**, 2-20 (1971).
2. Kuhn, J.R., Global Changes in the Sun, *The Structure of the Sun: VI Winter School at IAC*, T. Roca Cortes, F. Sanchez, eds. (Cambridge University Press, Cambridge) (1996).
3. Kuhn, J.R., Libbrecht, K.G., and Dicke, R. H., The Surface Temperature of the Sun and Changes in the Solar Constant, *Science* **242** 908-911 (1988).
4. Schur, W. and Ambronn, L., Messungen des Sonnendurchmessers *Astron. Mit. Koniglichen Stern. Zu Göttingen* 1-126 (1905).
5. Dicke, R. H. and Goldenberg, H. M., Solar Oblateness and General Relativity, *Phys. Rev. Letts.* **18** 313-316 (1967).
6. Hill, H.A. and Stebbins, R. T., The Intrinsic Visual Oblateness of the Sun, *Astrophys. J* **200** 471-483 (1975).
7. Dicke, R. H., Kuhn, J.R. and K. G. Libbrecht, Is the Solar Oblateness Variable? *Astrophys. J.* **318** 451-458 (1987).
8. Beardsley, B. The Visual Shape and Multipole Moments of the Sun, Ph.D. Thesis, Univ. Arizona, Tucson, AZ (1987).
9. Rösch, J., Rozelot, J.P., Deslandes, H., Desnoux, V., A New Estimate of the Quadrupole Moment of the Sun, *Solar Phys.*, **165** 1-11 (1996).
10. Lydon, T. J. and Sofia, S. A Measurement of the Shape of the Solar Disk, *Phys. Rev. Lett.* **76** 177-179 (1996).
11. Rozelot, J.P. and Rösch, J. An Upper Bound to the Solar Oblateness, *Solar Phys.* **172** 11-18 (1997).
12. Scherrer, P.H., et al. The Solar Oscillations Investigation – Michelson Doppler Imager *The SoHO Mission*, B. Fleck, V. Domingo, and A. Pollard, eds. (Kluwer, Holland) (1995).
13. Kuhn, J.R. et al., Precision Solar Astrometry from SoHO/MDI *IAU 181, Sounding Solar and Stellar Interiors*, G. Berthomieu, ed. (Kluwer, Holland)

(1997).

14. Lites, B., The extreme limb of the Sun, *Sol. Phys.* **85** 193-210 (1983).

15. Kuhn, J.R., Lin, H., and Loran, D, Gain Calibrating Nonuniform Image-Array Data Using Only the Image Data, *Publ. Astr. Soc. Pac.* **103** 1097-1108 (1991).

16. Ca II K images from the National Solar Observatory at Sacramento Peak were used to look for solar faculae and plage near the limb. The sun was very quiet during both MDI observations with only a single small plage region visible over the entire disk in both 1996 and 1997.

We wish to thank Julia Saba, Craig DeForest and Joseph Covington for their assistance in operating the MDI instrument during these observations. The efforts of Laura Allen, Helmut Schweitzer, Jean-Philippe Olive and Kelly Miller were essential in the planning and execution of the complicated SOHO roll maneuvers. The SOHO Flight Operations Team, including Harold Benefield, Nicholas Piston, and Brett Sapper made these activities run flawlessly. This work was supported by NASA. We wish to dedicate this paper to the memory of Robert H. Dicke (1916-1997), who inspired a generation of astrophysicists to consider the measurement and interpretation of the shape of the sun.

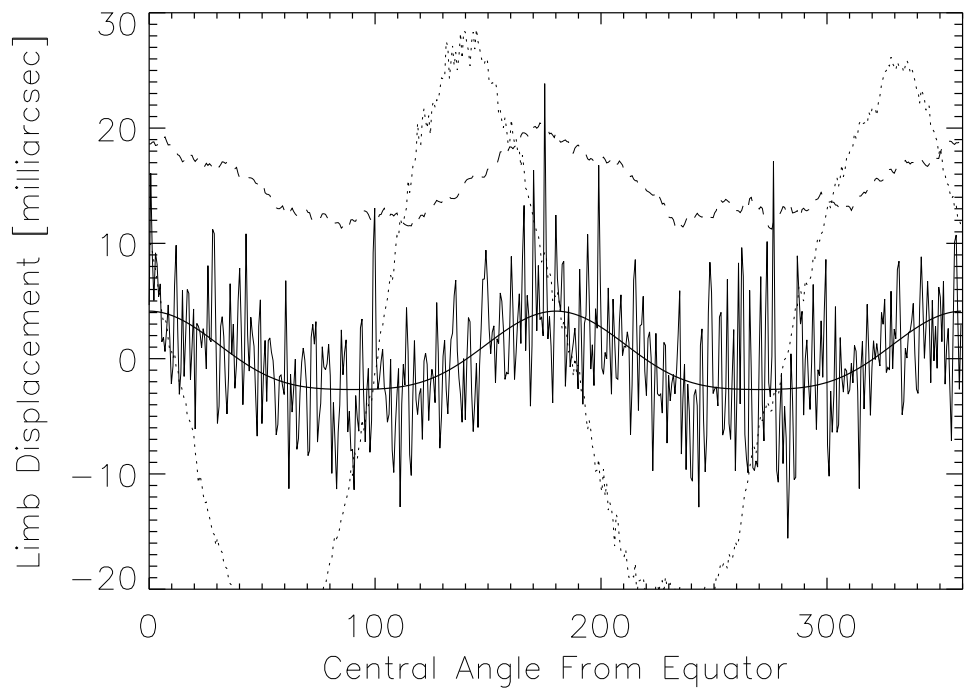
Figure Captions

Figure 1: This figure shows the limb displacement, $S(\theta)$, for each of the 512 angular bins around the sun as derived from 1997 measurements. From N evenly spaced roll angles distributed between 0 and 2π radians it can be shown that $\sum_k^N \alpha_k(\theta_i) \doteq NI_b(\theta_i)$ and $\sum_k^N \beta_k(\theta_i) \doteq NI_s(\theta_i)$. Here \doteq indicates that equality holds up to the $N - 1$ 'th angular harmonic component of α , β , I , S , and B . Once I_s and I_b are determined, the solar contributions, S and B , can be computed. With only 4 roll angles (spaced 90 degrees apart) the solar shape and brightness harmonic components with $l = 0, \dots, 3$ which vary as $\cos(il\theta)$ or $\sin(il\theta)$ are determined. Harmonics with $l = 0$ and 1 are filtered from the data because of their sensitivity to the scale (focus) and displacement (jitter) of the image. The plotted data were obtained by averaging the derived β coefficients from all of the roll positions, shifted into the solar reference frame. It is possible that the 4 milliarcsec rms high frequency noise that is apparent in the figure is due to residual photometric gain errors, and not solar limb structure, since both the 1996 and 1997 data were obtained near solar minimum, at a time when there was very little solar magnetic activity. Inspection of full disk Ca II K images¹⁶, obtained during a 3 day period around the time of the MDI data acquisition, reveals only quiet photosphere near the limb (except for a small plage region near position angle 20 degrees in 1996). The solid line shows our derived full resolution limb displacement in milliarcsec. The dashed line shows these data boxcar smoothed over a 22 degree interval (and offset by 15 milliarcsec). The dotted line shows the instrumental signal, $I_s(\theta)$, scaled by 0.05. The thick solid line shows the derived limb shape from the 3 term Legendre polynomial fit. Angles of 0, 90, 180 and 270 degrees correspond to the west, north, east, and south limbs.

Figure 2: The modern oblateness measurements versus time are plotted here

in terms of the fractional difference, ϵ , between the equatorial and polar solar radii, where $\epsilon = \frac{r_{equ} - r_{pole}}{R_{\odot}}$ and the apparent solar radius is $R_{\odot} = 972''$. While there is no evidence of an 11 or 22 year solar cycle trend, it is clear that the measurements and error limits have converged over the last decade toward the flattening implied by the surface photospheric solar rotation rate (as indicated by the dotted line). The symbols indicate the source reference for the plotted results: '-' - ref. 5, '*' - ref. 6, diamonds - ref. 7, large triangle - ref. 8, square - ref. 9, triangles - ref. 10, 'X' - this paper.

Figure 3: The effective limb temperature change versus position angle, θ , in 1997 is plotted here. The maximum limb brightness occurs near the equator and poles, with a temperature minimum occurring near 50 – 60 degrees north and south latitude (i.e. near position angles 55, 125, 235, and 305). The form of this latitudinal variation is nearly the same in both hemispheres although the amplitude of the modulation is larger in the southern hemisphere (about 2.2K versus 1.4K in the north). A pronounced 0.5K brightness dip within a few degrees of the south pole is also apparent in the data. It is notable that the temperature dip is not visible at the north pole, evidently because the north pole was inclined 6° out of the image plane, *away* from the earth.



Solar Oblateness Measurements

